Electron-electron interactions in GaAs-$Al_xGa_{1-x}As$ heterostructures

K. K. Choi* and D. C. Tsui
Department of Electrical Engineering, Princeton University, Princeton, New Jersey 08544

S. C. Palmateer†
General Electric Electronic Laboratories, Syracuse, New York 13221

(Received 6 January 1986)

Magnetoresistance measurements are made on the two-dimensional electron gas in GaAs-$Al_xGa_{1-x}As$ heterostructures as a function of the sample width (W) and the potential probe spacing (L) to study the electron-electron interactions. The temperature- (T) dependent parabolic magnetoresistance, observed above 0.1 T, clearly shows the effect of electron-electron interactions. When W is large compared with $L_T \equiv \pi(\hbar D/kT)^{1/2}$, the magnetoresistance agrees quantitatively with the two-dimensional (2D) interaction theory proposed by Altshuler and Aronov, confirming the earlier observations by Paalanen, Tsui, and Hwang. When $W \approx L_T$, a 2D-to-1D crossover is observed. For $W < L_T$, the magnetoresistance agrees quantitatively with the 1D interaction theory, if boundary scattering is negligible. When L is decreased and is less than $1.8L_T$, the zero-dimensional (0D) behavior is observed, confirming the 0D interaction theory. In the narrow channels, with W less than the elastic mean-free path (l_e), the orbital effects are greatly reduced by the boundary scattering, showing the precursor of the extremely 1D behavior. When the magnetic field is less than 0.1 T, a new size-dependent magnetoresistance is observed. This T-insensitive magnetoresistance is attributed to boundary scattering. In addition, when $L \approx L_T$, irregular conductance fluctuations of order e^2/h are observed, consistent with the recent theory of Lee and Stone on universal conductance fluctuations.

I. INTRODUCTION

The diffusive nature of electron motion in the hydrodynamic regime has been known for many years.[1,2] However, only recently, it was discovered that the interactions among these diffusing electrons may lead to significant modifications to the standard Fermi-liquid theory. The calculations based on perturbation theory in the weak-coupling regime, originally done by Altshuler and Aronov[3] and also by others,[4] show that most of the thermodynamic and kinetic quantities are modified, and often acquire singularities in two dimensions. Subsequently, Finkel'stein performed a renormalization-group analysis.[5,6] According to this analysis, when the Zeeman splittings are larger than kT or when magnetic impurities are present, the interaction increases with decreasing temperature (T) and at sufficient low T, drives a metallic system into the insulating regime. Castellani *et al.*[7] reached the same conclusion by a perturbative approach. On the other hand, in the absence of Zeeman splittings and magnetic impurities, Finkel'stein predicts a perfect conductor at $T=0$, while Castellani *et al.*[8] claim that the conductivity should remain finite at $T=0$.

Experimentally, there have been a number of attempts[9] to test the validity of the theory. While the experiments on the single-particle density of states,[10,11] the Hall coefficient,[12] and the electron-electron inelastic scattering time[13] can be understood within the framework of the interaction theory, direct determinations of the conductivity corrections[14–16] and the associated magnetoresistance[17,18] are still ambiguous. The ambiguity is due to the presence of other temperature-dependent mechanisms such as localization[19] and electron-phonon scattering.[14] In addition, the theory also predicts that there is a length scale governing the dimensionality of the electron-electron interactions. A change of the dimensionality should occur when the size of a sample approaches this length scale. So far, there is no experimental report on the existence of such a length scale, and the observation of the electron-electron interactions in different dimensions in a single system has not yet been realized.

In this paper we report our magnetoresistance measurements on the high-mobility two-dimensional electron gas (2DEG) in GaAs-$Al_xGa_{1-x}As$ heterostructures. The low-field parabolic magnetoresistance, already identified by Paalanen, Tsui, and Hwang[20] as due to the electron-electron interactions, is studied as a function of the sample width (W) and the potential probe spacing (L). The conductivity corrections ($\delta\sigma$), deduced from the magnetoresistance, are in good agreement with the interaction theory in two dimensions (2D), in one dimension (1D), and in zero dimension (0D), depending on W and L. The success of observing the interaction effect in all three dimensions in this system is attributed to its high mobilities. For example, with a mobility of $\approx 3\times 10^5$ cm^2/V s, the characteristic length governing the dimensionality of the interactions can be on the order of micrometers. Such micrometer-size devices can be conveniently fabricated, by using photolithographic techniques, to test the theory in different dimensions in a single system. In addition, only a small magnetic field (B) is needed to suppress the localization effect in these high-mobility samples. As a result,

the interaction effect can be studied unambiguously in a wide range of B.

This paper is organized into four sections. In Sec. II we review the theory of electron-electron interactions, emphasizing the fact that the interaction corrections to the conductivity of the 2DEG in GaAs-$Al_xGa_{1-x}As$ heterostructures can be measured directly from the parabolic magnetoresistance in all three dimensions. We also discuss briefly the effect of the boundary scatterings on the low-field magnetoresistance, and the universal conductance fluctuations in the magnetoresistance of small samples. In Sec. III we present our experimental results, some of which were reported earlier in Refs. 21 and 22. Discussions of the experiment and some concluding remarks are given in Sec. IV.

II. THEORETICAL BACKGROUND

A. Standard results

From the perturbation theory, there is a correction to the Drude conductivity (σ_0) due to the electron-electron interactions in the diffusion channel in the metallic regime ($E_F\tau/\hbar \gg 1$, τ is the impurity scattering time). When $kT\tau/\hbar < 1$, the theory[23,5] predicts in 2D,

$$\delta\sigma_{2D} = -\left[4-3\frac{2+F}{F}\ln\left[1+\frac{F}{2}\right]\right]\left[\frac{e^2}{2\pi^2\hbar}\right]\ln\left[\frac{\hbar}{kT\tau}\right], \tag{1}$$

where

$$F=\int\frac{d\theta}{2\pi}\left[1+\frac{2k_F}{\kappa}\sin\left[\frac{\theta}{2}\right]\right]^{-1}, \tag{2}$$

and κ is the inverse screening length in 2D.

When W is less than the thermal diffusion length (L_T), defined by $L_T \equiv \pi(\hbar D/kT)^{1/2}$, the interactions cross over to 1D. In this case,[19,24]

$$\delta\sigma_{1D} = -\left[\frac{4.91}{\pi}\left[1-12\frac{1+F/4-(1+F/2)^{1/2}}{F}\right]\right]\times\frac{e^2}{\sqrt{2}\pi^2\hbar W}L_T . \tag{3}$$

If the length of the channel (L) is also less than L_T, $\delta\sigma$ is given by the 0D theory,[25]

$$\delta\sigma_{0D} = -s\frac{e^2}{\sqrt{2}\pi^2\hbar W}L , \tag{4}$$

where s, the interaction constant, depends on the boundary condition. For a short channel with bulky metal contacts at the current leads,

$$s=\sqrt{2}\pi\left[0.36-\frac{1}{2}\left[1-\frac{1}{(1+F/2)^{1/2}}\right]\right].$$

In our experiments, we use long Hall bars and the length of the channel is defined by the potential probe spacing L. In this case, s can be shown to be

$$s=0.558\left[\frac{4.91}{\pi}\left[1-12\frac{1+F/4-(1+F/2)^{1/2}}{F}\right]\right].$$

The values in the large square brackets in Eqs. (1) and (3), and the parameter s in Eq. (4), can be deduced directly from experiment. For simplicity, we label these values by the interaction coefficients g_d, where d is the dimensionality. We compare the experimental g_d with those calculated from theory using F obtained from Eq. (2). The above results are obtained for short-range scatterers for which τ is the same as the transport time τ_{tr}. In general, if the range of the scattering potential is finite, the results are still correct provided that τ in the expressions of the conductivity corrections is replaced by τ_{tr}.[26]

In addition to the diffusion channel, there are corrections from the interactions in the Cooper channel. The functional form is the same as that given in Eqs. (1), (3), and (4), except that g_d is reduced by a factor of $1+g_d\ln(1.13E_F/kT)$,[27] where E_F is the Fermi energy and g_d is the appropriate bare interaction parameter in the Cooper channel. Concurrently, weak localization due to quantum interference also contributes to $\delta\sigma$. Reviews on these phenomena can be found in the articles by Lee and Ramakrishnan[4] and by Altshuler and Aronov.[9]

B. Derivation of $\delta\sigma$ in 1D and 0D

The rigorous results above are obtained from the current-current correlation function derived from the Kubo formula. The physical interpretation is not immediately apparent. Since the single-particle density of states was also found to be modified by the interactions in a similar way, it was thought that the corrections in the conductivity were due to the corrections in the density of states through Einstein's relation. However, Finkel'stein[5,6] emphasized recently that it is the compressibility $\partial N_s/\partial\mu$ that enters into Einstein's relation, $\sigma = e^2 D \partial N_s/\partial\mu$. (Here, N_s is the electron density and μ is the chemical potential.) Since there is essentially no diffusion correction to the compressibility, the conductivity correction comes from the modification of the diffusion coefficient D. Expressing $D = 1/2V_F^2\tau$ in 2D, we obtain a diffusion correction to the impurity scattering time τ, due to the electron-electron interactions. This is consistent with the calculations by Fukuyama[28] and the interaction correction to $\delta(1/\tau)/(1/\tau)$ in 2D shares the same functional form as $\delta\sigma/\sigma_0$. Following this argument, one can derive $\delta\sigma$ in 1D and 0D using a simplified formalism. Here, we briefly outline these calculations.

Following Fukuyama,[28] the contribution to the self-energy Σ from the process of Fig. 1 is given by

$$\Sigma(k,\epsilon_n) = -\frac{g}{\nu}T\sum_{\omega}\sum_{q}G(k+q,\epsilon_n+\omega_l)\Gamma^2(q,\omega_l,\epsilon_n) ,$$

$$G(k,\epsilon_n) = \left[i\epsilon_n - \frac{k^2}{2m}+\epsilon_F+\frac{i}{2\tau}\mathrm{sgn}\epsilon_n\right]^{-1}, \tag{5}$$

$$\Gamma(q,\omega_l,\epsilon_n) = \begin{cases}\tau^{-1}(Dq^2+|\omega_l|)^{-1} & \text{if } \epsilon_n(\epsilon_n-\omega_l)<0,\\ 0 & \text{otherwise},\end{cases}$$

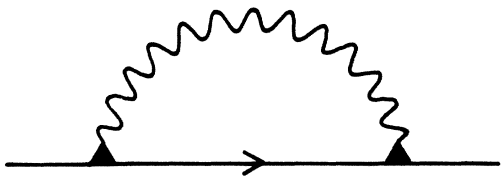

FIG. 1. Exchange self-energy correction due to electron-electron interactions.

where G is the thermal Green's function, and $\nu=m/2\pi\hbar^2$ is the single spin density of states of a Fermi gas. Since ω_l is order of $kT/\hbar$, when W is small so that $D(\pi/W)^2 > kT/\hbar$, the summation over q in Eq. (5) is limited to the q values in the direction of the length of the channel. When $W < \pi(\hbar D/kT)^{1/2}$, which is the thermal diffusion length L_T, we have

$$\Sigma(k,\epsilon_n) = -\frac{g}{\nu\tau^2} T \frac{1}{2\pi W} \sum_{\omega_l < -\epsilon_n} \frac{1}{i\epsilon_n + i\omega_l - i/2\tau} \times \int_{q_{\min}}^{q_{\max}} \frac{dq}{(Dq^2 + |\omega_l|)^2} , \tag{6}$$

where $q_{\min}$ and $q_{\max}$ are the momentum-transfer cutoff. $q_{\max}$ is set to $2\pi/\sqrt{D\tau}$, below which the diffusion approximation is valid. For a long channel, $q_{\min}=0$. For a short potential probe spacing L, the requirement that the diffusion interaction is valid within the spacing leads to $q_{\min} \geq 2\pi/L$. This limits the wavelength of the interaction potential to less than L. With these boundary conditions, and assuming $L > \pi(\hbar D/kT)^{1/2}$, we have

$$\int_{2\pi/L}^{2\pi/\sqrt{D\tau}} \frac{dq}{(Dq^2 + |\omega_l|)^2} = \frac{\pi}{4\sqrt{D}\,\omega_l^{3/2}} - \frac{2\pi}{L\omega_l^2} , \tag{7}$$

to the first order of $1/L$. If $L \to \infty$, by equating $\delta\sigma/\sigma_0 = \Sigma/(1/\tau)$, we have, from the first term of Eq. (7),

$$\delta\sigma = -g\frac{e^2}{\sqrt{2}\pi^2\hbar W} L_T . \tag{8}$$

If we include the effect of the Hartree interactions into the parameter g, and denote it by g_{1D}, Eq. (8) agrees with the more rigorous solution given by Eq. (3). If L is not too large compared with L_T, we have to include the second term in Eq. (7). In this case, we get

$$\delta\sigma = -g_{1D}\frac{e^2}{\sqrt{2}\pi^2\hbar W} L_T \left[1 - 1.79\frac{L_T}{L}\right] , \tag{9}$$

which agrees with the solution given in Ref. 25. On the other hand, when $L \ll L_T$, instead of Eq. (7) we have

$$\int_{2\pi/L}^{2\pi/\sqrt{D\tau}} \frac{dq}{(Dq^2 + |\omega_l|)^2} = \frac{L}{4\pi\omega_l D} .$$

Not surprisingly, $\delta\sigma$ in this case is given by

$$\delta\sigma = -g_{1D}\frac{e^2}{\sqrt{2}\pi^2\hbar W} aL , \tag{10}$$

where a is a constant given by

$$a = \frac{1}{2^{3/2}\pi} \sum_{l=0}^{\infty} \frac{1}{l+\frac{1}{2}} .$$

The value of a depends on the upper cutoff in ω_l. To estimate this value, we assume that the system crosses over from 1D to 0D smoothly as L changes. With this assumption, Eqs. (8), (9) and (10) can be combined in a single approximate formula,

$$\delta\sigma = -g_{1D}\frac{e^2}{\sqrt{2}\pi^2\hbar W}\left[\frac{1}{L_T} + \frac{1.79}{L}\right]^{-1} . \tag{11}$$

It implies that a in Eq. (10) is 0.558, a value that can be determined by experiment. According to Eq. (11), when the correction to the conductivity is dominated by the electron-electron interactions, the effective length scale (L_{eff}) is, in general, given by

$$\frac{1}{L_{\text{eff}}} = \frac{1}{L_T} + \frac{\alpha}{L} , \tag{12}$$

where $\alpha = g_{1D}/s$, a constant dependent on the boundary conditions. This is in contrast to the effective length scale expected from the localization theory,[29] which predicts

$$\frac{1}{L_{\text{eff}}^2} = \frac{1}{L_i^2} + \frac{1}{L^2} , \tag{13}$$

where L_i is the inelastic scattering length. Hence, by comparing the length-scale dependence, one can distinguish the interaction effect from the localization effect. Masden and Giordano[15] performed a systematic measurement on the length-dependent resistance of thin $Au_{40}Pd_{60}$ wires. They found that the length-scale dependence is consistent with Eq. (12) instead of Eq. (13) expected from the localization theory. According to the above analysis, it is evident that the phenomenon observed by Masden and Giordano is dominated by the electron-electron interactions.

C. Magnetoresistance

The use of resistance measurements to determine electron-electron interactions is not a straightforward task. For example, the quantum corrections to the resistivity as a function of T have to be extracted from a T-dependent background which is due to classical effects such as electron-phonon scattering[14] and the T-dependent Coulomb scattering by individual ionized impurities.[30] In addition, all three quantum corrections, i.e., localization, the electron-electron interactions in the Cooper channel, and the electron-electron interactions in the diffusion channel share the same T dependence.

In principle, the quantum corrections can be separated by applying a magnetic field since each quantum effect has a different B dependence. In practice, however, a combination of different B dependences can be complicated in most systems, hampering a clear demonstration of the individual effects. Fortunately, for the high-mobility 2DEG in GaAs-$Al_xGa_{1-x}As$ heterostructures, there ex-

ists a range of B that shows preferentially the effect of the electron-electron interactions in the diffusion channel. One can take advantage of this fact to study the electron-electron interactions. In the following, we briefly review the magnetoresistance due to the various quantum effects.

It is well established that there is a negative magnetoresistance associated with the weak localization effect.[19,31] In 2D,

$$\delta\sigma(B)-\delta\sigma(0)=\frac{e^2}{2\pi^2\hbar}\left[\psi\left[\frac{1}{2}+\frac{1}{a\tau_i}\right]-\psi\left[\frac{1}{2}+\frac{1}{a\tau}\right]+\ln\left[\frac{\tau_i}{\tau}\right]\right], \tag{14}$$

where τ_i is the inelastic scattering time or phase relaxation time, $a=4DeB/\hbar$, and ψ is the digamma function. The effect of B is to suppress localization. It can be shown[32] that when the magnetic length of the Cooper propagator ($\sqrt{\hbar/2eB}$) is less than the elastic mean free path (l_e), localization will be totally suppressed. In other words, when $B>\hbar/2el_e^2$ (≈ 1 G for our device with mobility 3×10^5 cm^2/V s), the localization effect can be ignored.

For the electron-electron interactions in the Cooper channel in 2D, the effect of B can be written as[27]

$$\delta\sigma(B)-\delta\sigma(0)=-\frac{e^2}{2\pi^2\hbar}g(T)\phi_2\left[\frac{2eDB}{\pi T}\right]-\frac{e^2}{2\pi^2\hbar}\beta(T)\left[\psi\left[\frac{1}{2}+\frac{1}{a\tau_i}\right]-\psi\left[\frac{1}{2}+\frac{1}{a\tau}\right]+\ln\left[\frac{\tau_i}{\tau}\right]\right], \tag{15}$$

where

$$\phi_2(x)=\int_0^\infty \frac{t\,dt}{\sinh^2 t}\left[1-\frac{xt}{\sinh(xt)}\right],$$

$$g^{-1}(T)=(g_d)^{-1}+\ln\left[\frac{1.13E_F}{kT}\right],$$

$$\beta(T)=\frac{\pi^2}{4\ln(T/T_c)}.$$

Here, T_c is the superconducting transition temperature. When the interaction is repulsive, the magnetoresistance is positive. However, in this case, the interaction enhances the zero-field conductivity.[9] Hence, the B field still suppresses the interaction effect in the Cooper channel. Although the B dependence of the first term differs from localization, it can be deduced from the derivation of Eq. (15) in Ref. 27 that the B field required to suppress the first term is also the same as that for localization. Therefore, for high-mobility samples, there is no contribution to the conductivity from the effects associated with the Cooper propagators above a few gauss. This is also true for other dimensions.

In contrast to the B sensitivity of the Cooper propagators, there is no magnetic effect on the interactions in the diffusion channel, even at $\omega_c\tau\gg1$,[33] until the energy associated with the spin becomes important. In this case, the 2D magnetoconductance[34] associated with the diffusion channel is given by

$$\delta\sigma(B)-\delta\sigma(0)=-\frac{e^2}{\hbar}\frac{\Xi}{4\pi^2}g_2(h), \tag{16}$$

where

$$\Xi=4\left[\frac{2+F}{F}\right]\ln(1+F/2)-4,$$

$$g_2(h)=\int_0^\infty d\Omega\frac{d^2}{d\Omega^2}[\Omega N(\Omega)]\ln\left|1-\frac{h^2}{\Omega^2}\right|,$$

$$h=g^*\mu_B B/kT,$$

and

$$g_2(h)=\begin{cases}\ln(h/1.3) & \text{if } h\gg1,\\ 0.084h^2 & \text{if } h\ll1.\end{cases}$$

Ξ is the interaction parameter of the $|S_z|=1$ triplet contribution. We expect that a positive magnetoresistance will be observed when $h\approx1$. In our samples, B corresponds to 4.3 T (Ref. 35) when $T\approx1.5$ K. Since the interaction in the diffusion channel decreases the conductivity, the magnetic field in this case enhances the interaction. However, when $B\ll4.3T$, this enhancement is negligible.

Now, we have for our samples a particularly simple situation in the range of B from a few gauss to 1 T. In this range, the only quantum contribution to the conductivity is from the interactions in the diffusion channel. It is unchanged under the applied field and is given by the zero-field expressions Eqs. (1), (3), and (4). In our experiment, the device has a Hall-bar geometry. When B is applied, the measured quantity is ρ_{xx} instead of σ_{xx}. To calculate the change in ρ_{xx}, we notice that $\delta\sigma_{xy}=0$ (Ref. 33) in all dimensions for the interaction effects in the diffusion channel. By inverting the conductivity tensor, we obtain, in the presence of the Shubnikov–de Haas (SdH) oscillations,[36]

$$\rho(B)=\rho_0+[1+(\omega_c\tau)^2]\frac{\sigma_s}{\sigma_0^2}-[1-(\omega_c\tau)^2]\frac{\delta\sigma_i}{\sigma_0^2}, \tag{17}$$

where

$$\rho_0=\sigma_0^{-1},$$

$$\sigma_s=-\frac{\sigma_0}{1+(\omega_c\tau)^2}2\frac{(\omega_c\tau)^2}{1+(\omega_c\tau)^2}\frac{2\pi^2kT}{\hbar\omega_c}\times\operatorname{csch}\left[\frac{2\pi^2kT}{\hbar\omega_c}\right]\cos\left[\frac{2\pi E_F}{\hbar\omega_c}\right]e^{-\pi/\omega_c\tau}.$$

Here, σ_0 is the Drude conductivity, σ_s contains the SdH

oscillations, and $\delta\sigma_i$ is the interaction contribution given by Eqs. (1)—(4). It is clear from the first term of Eq. (17) that there is no classical magnetoresistance associated with the Drude conductivity. The second term indicates that the amplitude of the SdH oscillations increases exponentially once $\hbar\omega_c > kT$ and $\hbar/\tau$. The third term is the parabolic negative magnetoresistance from the interaction effect. Here, we should emphasize that this magnetoresistance is a classical orbital effect which depends only on the perpendicular component of B.

According to Eq. (17), when $B=0$, $\rho(0)=\rho_0-\delta\sigma_i/\sigma_0^2$. Since $\delta\sigma_i<0$, the interactions increase the resistivity at zero field, and the magnetoresistance $\Delta\rho(B)$, defined as $\rho(B)-\rho(0)$, is given by

$$\Delta\rho(B)=\frac{(\omega_c\tau)^2}{\sigma_0^2}\delta\sigma_i+[1+(\omega_c\tau)^2]\frac{\sigma_s}{\sigma_0^2} .$$

Since σ_s is an oscillating function, it does not contribute to the monotonic magnetoresistance, and consequently, even when the SdH oscillations are present, the interaction effects can be deduced from the background magnetoresistance by joining the midpoints of the oscillations. The monotonic term can be written as

$$\Delta\rho(B)=\left[\frac{e\tau}{m\sigma_0}\right]^2 B^2\delta\sigma_i . \tag{18}$$

In the range of B of interest, $\delta\sigma_i$ is constant and Eq. (18) predicts a parabolic magnetoresistance. By measuring $\Delta\rho/B^2$, we can obtain $\delta\sigma_i$ regardless of the dimensionality of the sample.

The present experiment is designed to determine $\delta\sigma_i$ in samples with different sizes relative to L_T, by measuring the magnetoresistance. Our results are compared with the predictions in 2D, 1D, and 0D. Before entering the discussion of these results, we wish to review briefly the effect of boundary scattering on the magnetoresistance, and the conductance fluctuations expected in small samples. These phenomena are not from the electron-electron interactions; they are observed in our samples with L and W around a few micrometers.

D. Boundary scattering

Equation (18) can be rewritten as

$$\Delta\rho(B)=\frac{1}{N_s^2e^2}\left[\frac{\tau_L}{\tau_{\rm tr}}\right]^2 B^2\delta\sigma_i . \tag{19}$$

Here, we differentiate the lifetime τ_L of an electron in a Landau orbit and the transport $\tau_{\rm tr}$ deduced from the conductivity. When they are the same,

$$\Delta\rho(B)=\frac{1}{N_s^2e^2}B^2\delta\sigma_i . \tag{20}$$

However, when W is comparable to l_e, the scattering of electrons by the sample boundaries can play an important role. More specifically, the boundary scattering is just as effective as the impurity scattering in limiting τ_L, but its effect on the conductivity depends on whether the scattering is diffusive or specular. By comparing the resistivity of narrow channels with that of wide channels, we concluded that the latter dominates in our samples. As a result, τ_L is expected to be less than $\tau_{\rm tr}$ and the measured magnetoresistance is expected to be smaller than that predicted by Eq. (20). Indeed, the increasing importance of the boundary scattering as W decreases can be viewed as the precursor of the extremely 1D case in which the electrons are also bound along the width. In this extremely 1D limit, the orbital effect we have discussed should be quenched completely. Therefore, in the absence of a more detailed theoretical analysis in this regime, the use of Eq. (20) to determine the interaction parameters in our extremely small channels cannot be quantitatively correct. Although it is still useful in demonstrating the functional dependence of the interaction effects, the interaction parameters deduced from it will be reduced.

In our experiment, we also observed a T-insensitive parabolic magnetoresistance in narrow channels ($W\leq 3$ μm) when $B\leq 0.1$ T. This size-dependent magnetoresistance is also attributed to the boundary scattering and it will be discussed in Sec. III.

E. Universal conductance fluctuations

It is well known that large fluctuations appear in the measurements of small samples.[37—39] Some fluctuations, recently discussed by Lee and Stone and also by Altshuler,[40,41] are results of the highly correlated electron paths in space due to quantum diffusion. They found that at $T=0$ the amplitude of the fluctuations in the conductance as a function of chemical potential or B is of the order of e^2/h, independent of the sample size, shape, and the conductance itself. It is related to the sample size at finite T because such fluctuations are apparent only when $L<L_T$ or L_i (where L_i is the inelastic mean free path). In this case, ensemble averaging cannot be performed. The fluctuations, hence, result from the fact that the conductance associated with each electron path of definite energy is different.

III. EXPERIMENTAL RESULTS

In order to test the theory of electron-electron interactions in different dimensions, we fabricated about twenty samples with different combinations of L and W from two modulation-doped GaAs-$Al_xGa_{1-x}As$ wafers. Conventional photolithographic techniques are used to define the Hall-bar pattern for four terminal measurements. Here, we present the representative data from ten samples. The sample parameters and specifications are shown in Table I. The first six samples are fabricated from the same wafer which has an average $N_s\approx 5\times 10^{15}$ m^{-2} and an average mobility $\mu\approx 2.5\times 10^{15}$ cm^2/V s. The other four samples are fabricated from the other wafer with $N_s\approx 4.6\times 10^{15}$ m^{-2} and $\mu\approx 1.8\times 10^5$ cm^2/V s. At $T=2$ K the samples from the first wafer have $L_T\approx 4.1$ μm and those from the second have $L_T\approx 3.4$ μm. Since these length scales are comparable to the physical dimensions of the samples listed, we expect a dimensional crossover to occur when the temperature is decreased below 4.2 K. In Table I, we also list the theoretical crossover temperatures

TABLE I. Sample parameters and the theoretical dimensional crossover temperatures.

Sample no	W (μm)	L (μm)	N_s (10^{15} m^{-2})	τ (10^{-12} s)	T_{c1} (K)	T_{c2} (K)
1	156	338	5.03	11.4	0.0017	
2	34.5	272	5.43	9.68	0.031	
3	6.2	272	5.02	11.3	1.1	
4	3.5	310	5.43	9.68	3.0	
5	3.0	272	4.79	7.45	2.9	
6	1.1	272	4.84	10.3	28	
7	2.7	59	4.60	7.15	3.2	0.02
8	3.0	7.5	4.78	6.88	2.6	1.3
9	1.9	6.2	4.60	7.15	6.5	1.9
10	2.6	6.7	4.91	7.12	3.7	1.8

T_{c1} and T_{c2}. The former is the 2D-to-1D crossover temperature at which $L_T(T_{c1})=W$, and the latter is the 1D-to-0D crossover temperature, defined in Eq. (11), at which $L_T(T_{c2})=L/1.79$. The magnetoresistance data are recorded between 1.25 and 8 K with a perpendicular magnetic field up to 0.8 T. The measurements are made using a lock-in amplifier at 145 Hz and a constant-current source of 10^{-8} A to avoid electron heating.[42]

Figure 2 shows the magnetoresistance data for a wide sample (no. 1) and for three narrow and long samples (nos. 3, 5, and 6), previously reported in Ref. 21. Figure 3 shows the data from a narrow but short sample, with $W=1.9$ μm and $L=6.2$ μm, at 4.2 and 1.25 K. The inset shows the sample geometry. These data illustrate the change in the perpendicular field magnetoresistance as we vary W and L. In the wide channel ($W=156$ μm), the parabolic magnetoresistance is observed from $B=0.02$ T to approximately 0.4 T, confirming the earlier observations made by Paalanen, Tsui, and Hwang.[20] When the width of the channel becomes small ($W\approx 6.2$ μm), parabolic magnetoresistance can be identified in two regimes with a critical field (B_c) around 0.1 T. Below B_c, the magnetoresistance is insensitive to temperature, in contrast to the magnetoresistance at higher fields, which is temperature dependent. As the width of the channel decreases further, the magnitudes in both regimes increase and B_c extends to higher fields. For a 1.1-μm-wide channel, B_c increases to 0.25 T. At lower temperatures (1.6 K), the SdH oscillations become apparent. Strikingly, the onset of the oscillations depends on the sample size, although the mobility of the samples is approximately the same. For very narrow channels (no. 6 in Fig. 2 and no. 9 in Fig. 3), in addition to the SdH oscillations, irregular, aperiodic, and T-insensitive fluctuations are observable below 0.5 T. Here, we note that the magnetoresistance observed in a parallel magnetic field is less than 0.1% of that in the perpendicular field case. This fact shows that all the aforementioned magnetic effects up to 0.8 T are orbital in nature.

A. Magnetoresistance below B_c

An example of the magnetoresistance below B_c is shown in Fig. 4, where it is plotted against B^2 from 0 to 0.055 T for sample no. 4 ($W=3.5$ μm). For $B<0.01$ T,

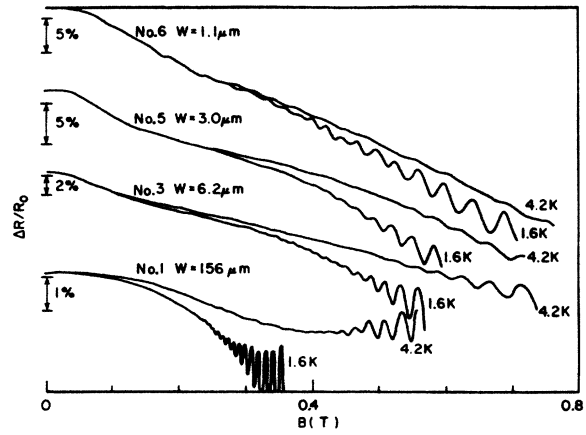

FIG. 2. Change of resistance, $\Delta R/R_0$, as a function of perpendicular field at 4.2 and 1.6 K. The irregular structures in the data of sample no. 6 below 4 kG are reproducible; they are not Shubnikov–de Haas oscillations.

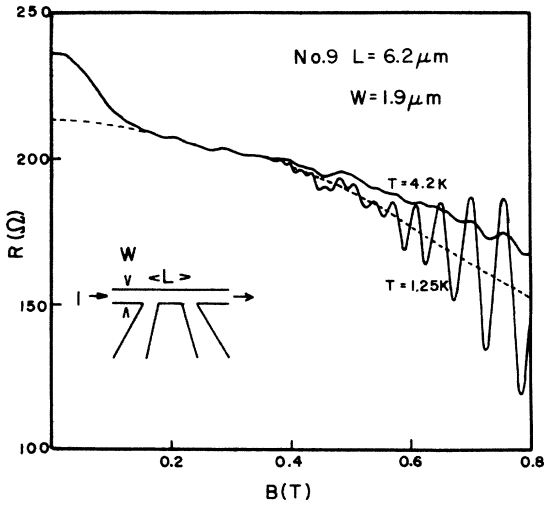

FIG. 3. Magnetoresistance of sample no. 9 with $W=1.9$ μm, $L=6.2$ μm at $T=4.2$ K (upper curve), and $T=1.25$ K (lower curve). The dashed line is the extrapolation of the B^2 dependence above B_c at $T=4.2$ K to zero field. The y intercept gives the magnitude of the T-insensitive magnetoresistance.

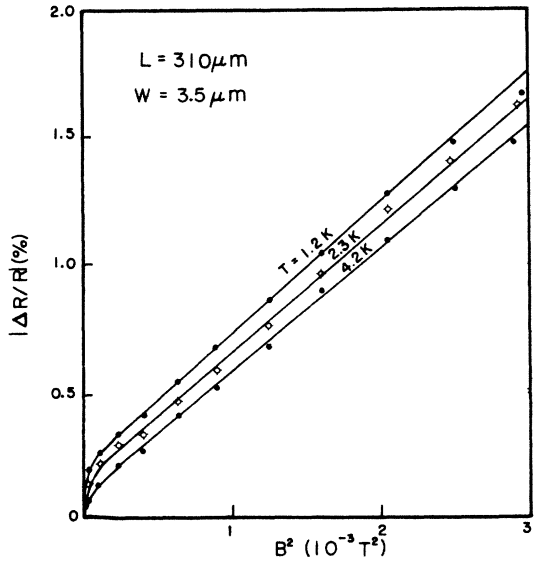

FIG. 4. Change of resistance, $\Delta R/R_0$, of sample no. 4 with $W=3.5\ \mu$m, $L=310\ \mu$m against B^2 from 0 to 550 G.

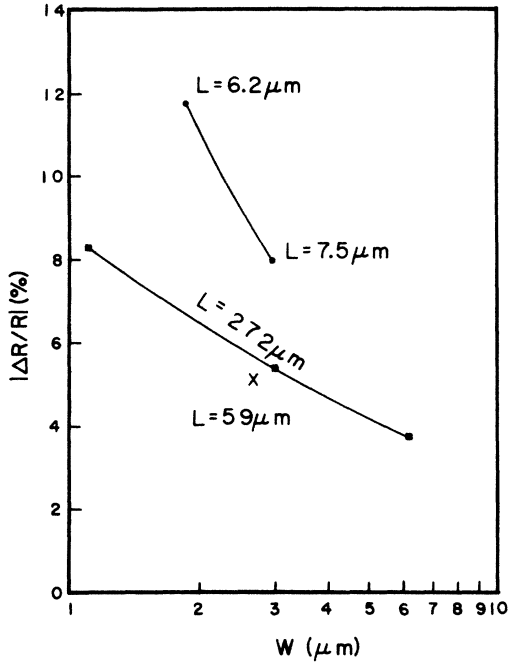

FIG. 6. Temperature-insensitive part of the magnetoresistance below 0.15 T from seven devices. W is the sample width and L is the potential probe spacing.

the magnetoresistance is caused by the magnetic effect on the Cooper propagators mentioned in the preceding section. This T-dependent magnetic effect is now under investigation, and it will not be discussed further in this paper. For $B\approx 0.01$ to 0.05 T the magnetoresistance is linear in B^2 and the slope is independent of T below 4.2 K. This approximately parabolic magnetoresistance is size dependent. However, it is not caused by the electron-electron interactions for the following two reasons. First, it is almost temperature independent, contrary to the predictions from either the 2D or the 1D interaction theory. Second, a fit of the 4.2-K data to Eq. (3) yields $g_{1D}\approx 11.6$, an order of magnitude higher than that expected from the interaction theory.

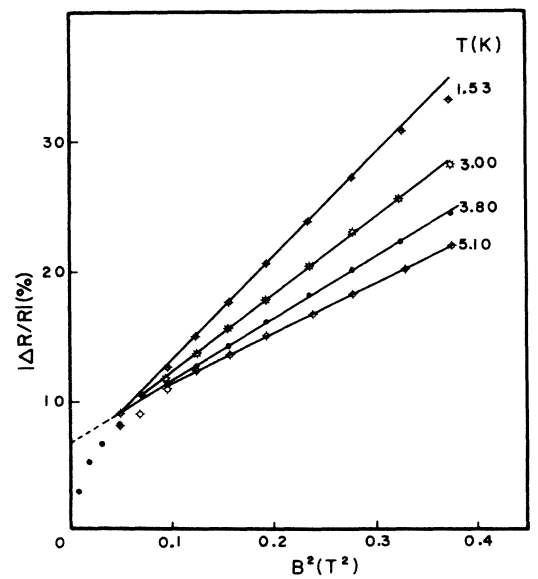

FIG. 5. Change of the resistance, $\Delta R/R_0$, of sample no. 4 with $W=3.5\ \mu$m against B^2 from 0 to 0.6 T. The dashed line is the extrapolation of the B_c dependence above B_c at $T=3.8$ K to zero field.

The magnetoresistance deviates from the B^2 dependence as B approaches B_c (≈ 0.1 T in Fig. 3), and vanishes at higher B. When B is well above B_c, the T-dependent parabolic magnetoresistance becomes dominant (Figs. 2, 3, and 5). If we assume that the B^2 dependence above B_c can be extrapolated at each temperature to below B_c, as indicated by the dashed line for $T\approx 4.2$ K in Figs. 3 and 5, we can obtain the magnitude of the magnetoresistance below B_c from the y intercept of the dashed line. The magnitude is slightly dependent on the temperature. In Fig. 6 we summarize our data on this magnitude as a function of the sample size for seven samples at 4.2 K. It shows that this T-insensitive, negative magnetoresistance is larger for smaller L or W.

We attribute this conductivity enhancement to the skipping orbits in a restricted geometry. For the samples we used, the elastic mean free path is around 3 μm, which is comparable or even larger than the size of the samples shown. Here, the boundary scattering plays an important role. At zero magnetic field, the scattering between the electrons and the boundaries is essentially specular and does not affect the conductivity. This can be verified by comparing the conductivity of the wide and narrow samples. However, due to their high mobilities, the transports in these samples switch from the weak-field limit ($\omega_c\tau<1$) to the classical high-field limit ($\omega_c\tau>1$) in a rel-

atively low-field regime (≈ 0.04 T). In this "high"-field limit, scattering sites are needed for current transport. The boundaries in this case provide additional scattering sites for the current transport and hence decrease the resistivity. The magnetoresistance begins to saturate when the electrons are able to complete cyclotron orbits in higher fields instead of executing skipping orbits. For a channel 1.5 μm wide, the magnetoresistance should begin to saturate when $d_H \approx 1.5$ μm, where d_H is the diameter of the cyclotron orbit. In other words, B_c should be around 0.15 T, consistent with the experimental result. According to this argument, the decrease in the resistivity is proportional to the boundary scattering rate and hence inversely proportional to the width. Also, the model correctly explains the weak temperature dependence of the magnetoresistance in this regime since all the parameters involved are temperature independent. Indeed, the magnetoresistance decreases only by 12% at $T=10$ K and 48% at 20 K.

Another evidence for the important role played by the boundary scattering in the narrow channels is the additional broadening of the Landau levels. The boundary scattering reduces the lifetime (τ) of an electron in a Landau orbit and hence the criterion $\omega_c \tau > 1$ in Eq. (17) is satisfied at higher fields. This leads to the SdH oscillations emerging at higher fields for narrower channels, as shown in Fig. 2.

B. Fluctuations in magnetoresistance

For samples nos. 6 and 9, the fluctuations observable below 0.5 T are not SdH oscillations. These fluctuations are aperiodic and T insensitive. Although the fluctuations of samples nos. 6 and 9 look similar, they actually correspond to very different fluctuations in the conductance G. This can be seen by expressing ΔG as $\Delta R/R^2$ for small ΔG. For similar fluctuations in $\Delta R/R$, ΔG is inversely proportional to the resistance of the entire channel. Numerically, the fluctuations in the conductance for sample no. 9 are from $0.7e^2/h$ to $1.8e^2/h$, whereas the ΔG for sample no. 6 are only from $0.014e^2/h$ to $0.064e^2/h$, much smaller than that of sample no. 9. These quantities are consistent with the theory proposed by Lee and Stone.[40] The fluctuations reveal the fundamental transport characteristics of a sample when $L \leq L_T$. For sample no. 9, this condition is satisfied and the order of the fluctuations is e^2/h. On the other hand, the length of sample no. 6 is much larger than $L_T \approx 4$ μm, rendering the fluctuations small.

C. Magnetoresistance above B_c

The magnetoresistance above B_c is caused by the electron-electron interactions. To verify this, the magnetoresistance of samples nos. 4 and 9 is plotted against B^2, from 0 to ≈ 0.7 T, in Figs. 5 and 7, respectively. The magnetoresistance is T dependent and is linear in B^2. From the slopes of these curves, $\Delta\rho(B)/B^2$ at different temperatures can be extracted and compared with the theory. In 2D, when $kT\tau_{\rm tr}/\hbar \geq 1$, which is the case here, Eq. (1) cannot be directly applied. Instead, we use the more general expression[28]

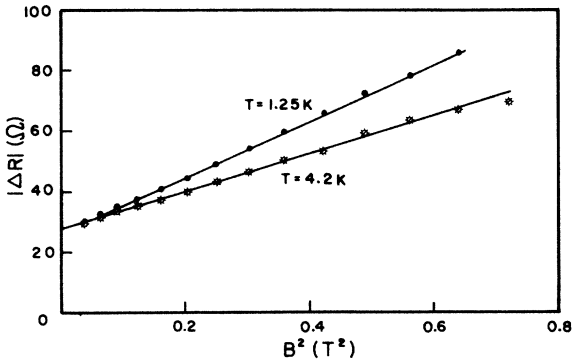

FIG. 7. Change of resistance, ΔR, of the sample no. 9 against B^2. The curves are linear up to 0.8 T.

$$\delta\sigma_{\rm 2D} = -\frac{e^2}{2\pi^2\hbar} g_{\rm 2D} \left[\psi\left(\frac{1}{2} + \frac{\hbar}{kT\tau_{\rm tr}} \right) - \psi\left(\tfrac{1}{2}\right) \right], \quad (21)$$

where ψ is the digamma function. When $kT\tau_{\rm tr}/\hbar \ll 1$, Eq. (1) is recovered. According to Eqs. (20) and (21),

$$\Delta\rho(B) = -\frac{1}{N_s^2} \frac{1}{2\pi^2\hbar} g_{\rm 2D} \left[\psi\left(\frac{1}{2} + \frac{\hbar}{kT\tau_{\rm tr}} \right) - \psi\left(\tfrac{1}{2}\right) \right] B^2 \quad \text{for 2D} . \quad (22)$$

Also, from Eqs. (3) and (19),

$$\Delta\rho(B) = -\frac{1}{N_s^2} \frac{1}{\sqrt{2\pi\hbar W}} g'_{\rm 1D} \left(\frac{\hbar D}{kT} \right)^{1/2} B^2 \quad \text{for 1D} , \quad (23)$$

and

$$\Delta\rho(B) = -\frac{1}{N_s^2} \frac{0.558}{\sqrt{2\pi^2\hbar W}} g'_{\rm 1D} L B^2 \quad \text{for 0D} . \quad (24)$$

Here, $g'_{\rm 1D}$ is defined by

$$g'_{\rm 1D} = \left(\frac{\tau_L}{\tau_{\rm tr}} \right)^2 g_{\rm 1D} , \quad (25)$$

the apparent interaction parameter in 1D deduced from the orbital magnetoresistance. Equations (22)—(25) hold for both short- and long-range scatterers.[26]

In order to facilitate comparison with the 2D theory expressed by Eq. (22), we plot in Fig. 8 the data from the four wider samples (nos. 1—4) in the parabolic regime as $|\Delta\rho(B)/B^2| N_s^2 2\pi^2\hbar$ versus $\psi(\frac{1}{2}+\hbar/kT\tau_{\rm tr}) - \psi(\frac{1}{2})$. For samples with $W=156$ and 34.5 μm, respectively, the data follow two straight lines passing through the origin, as expected from the 2D theory. From their slopes, we obtain $g = 0.54 \pm 0.02$ and 0.51 ± 0.02. These values of g are close to the theoretical value of 0.7 for $F=0.45$, calculated from Eq. (2) using $N_s \approx 5 \times 10^{15}$ m^{-2}. Within the experimental uncertainties, the data show no W dependence, consistent with Eq. (1). For $W=6.2$ and 3.5 μm, the data show increasing deviations from the 2D behavior as T decreases. These deviations are suggestive of a transition as T approaches T_{c1} (Table I), expected for the cross-

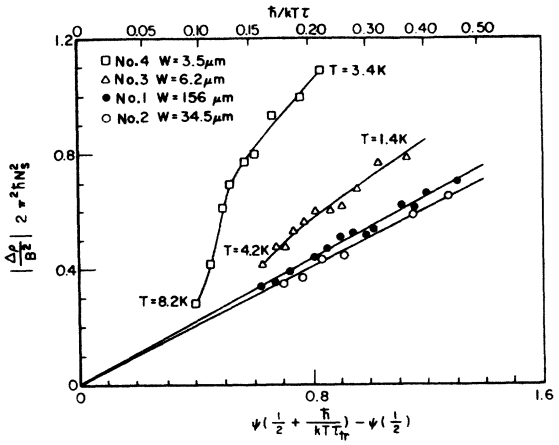

FIG. 8. $|\Delta\rho/B^2|\,2\pi^2\hbar N_s^2$ vs $\psi(\frac{1}{2}+\hbar/kT\tau_{tr})-\psi(\frac{1}{2})$ for samples nos. 1–4.

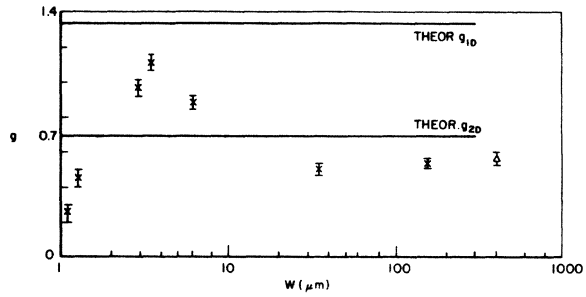

FIG. 10. Experimental values of the interaction parameter g vs W. g is extracted either from Eq. (22) or from Eq. (23) as determined by the characteristic temperature dependence of $\delta\sigma$. Since g is a weak function of N_s, the data show only the general trend. The data point (Δ) is from Ref. 20 with $N_s=1.17\times10^{15}$ m^{-2}, from Eq. (22).

over from the 2D interaction effect to 1D interaction effect.

In Fig. 9 the data from the four narrower samples (nos. 3–6) are plotted as $|\Delta\rho(B)/B^2|$ versus $1/\sqrt{T}$. For $W=1.1$ μm, the $1/\sqrt{T}$ dependence, predicted by the 1D interaction theory [Eq. (23)], is observed in the entire T range. For $W=3.0$ and 3.5 μm, this T dependence is observed when $T<T_{c1}$, whereas for $W=6.2$ μm the 1D characteristics are not yet fully developed, consistent with the predicted T_{c1} of 1.1 K. In addition, $|\Delta\rho|$ is observed to increase with decreasing W for $W\geq3$ μm, consistent with the expected $1/W$ dependence. The g values, deduced from the slopes of the curves using Eq. (23), are as shown in Fig. 10, together with those of samples nos. 1 and 2 obtained from the 2D theory using Eq. (22). The largest value of g, obtained from the 3.5-μm-wide channel, is 1.11 ± 0.05, close to the theoretical value $g_{1D}=1.33$, calculated from Eq. (2) using $F=0.45$. For the 6.2-μm-wide channel, g deduced from the data at $T=1.5$ K is 0.89, indicating that the sample is in a 2D-to-1D transition in this temperature range. For $W<3.5$ μm, the apparent value of g begins to drop. In this W range, the width of the sample is comparable to the elastic mean free path ($l_e\approx3$ μm). As mentioned before, a direct comparison with the theoretical g value cannot be made. Instead, from Eq. (25), we expect the experimental g value to decrease as W^2 since τ_L due to boundary scatterings is approximately proportional to W. This is roughly what was observed, and the value of g obtained from the 3.5-μm-wide channel may already be reduced from its theoretical value. In any case, a more quantitative theory is needed to elucidate this aspect of our data. Here, we simply point out that the decrease of g indicates once again the important role of boundary scattering in narrow channels on the orbital magnetic effects.

Next, we investigate the L dependence of the magnetoresistance of narrow channels. In Fig. 11 the data from the four narrow samples with different potential probe spacings are shown. For sample no. 7, with $W=2.7$ μm and $L=59$ μm, the 1D behavior is observed below T_{c1}. For sample no. 8, with $L=7.5$ μm, the magnitude of $\Delta\rho/B^2$ ceases to increase below $T=1.4$ K indicative of a dimensional crossover from 1D to 0D. As L is reduced further to 6.7 and 6.2 μm, the crossover occurs at higher

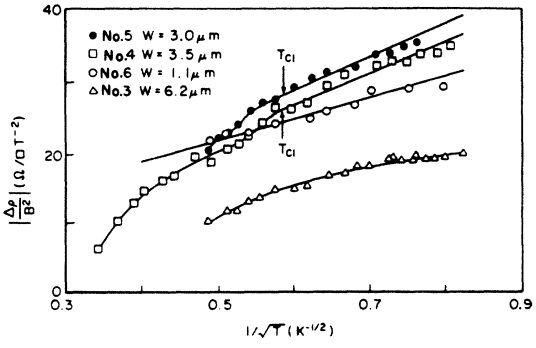

FIG. 9. $|\Delta\rho/B^2|$ vs $1/\sqrt{T}$ for samples nos. 3–6.

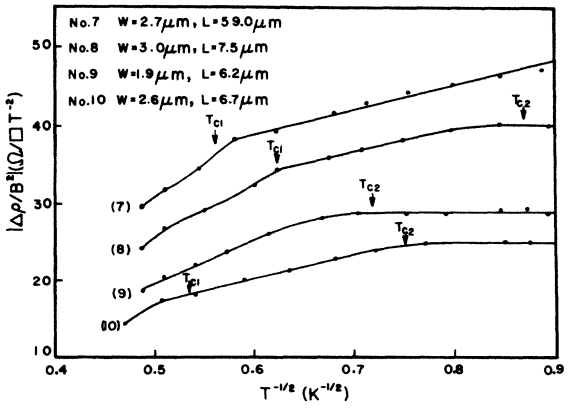

FIG. 11. Plot of $|\Delta\rho/B^2|$ vs $1/\sqrt{T}$ for samples nos. 7–10. T_{c1} and T_{c2} are the predicted 2D-to-1D and 1D-to-0D crossover temperatures, respectively, calculated from the geometry of the samples.

temperatures, consistent with Eq. (11). The crossover temperatures T_{c1} and T_{c2} indicated in the figure are the theoretical values, calculated from the geometry of the samples according to $L_T(T_{c1})=W$ and $L_T(T_{c2})=L/1.79$, the criteria for the 2D-to-1D crossover and 1D-to-0D crossover, respectively. Therefore, a two-dimensional sample at high temperatures may undergo a sequence of dimensional crossovers as T decreases and finally becomes a zero-dimensional sample at sufficiently low T as far as the interaction effect is concerned.

The value of g_{1D} can be extracted from the saturation value of $\Delta\rho/B^2$ using the 0D expression given by Eq. (24). From samples nos. 8, 9, and 10, we obtain $g'_{1D}=0.96$, 0.64, and 0.49, respectively. These values agree with those deduced from the slopes of the same curves, before saturation, using the 1D theory to within 10—30%. It shows the consistency between theory and experiments and verifies the validity of Eq. (11).

IV. DISCUSSION AND CONCLUSION

In the preceding section we saw the agreement between the predictions of the interaction theory and the experimental data. This agreement is a direct confirmation that the electron-electron interactions play an important role in this system. The interaction theory correctly predicts that there is a temperature-dependent parabolic magnetoresistance. From this magnetoresistance, the corrections to the conductivity due to the electron-electron interactions can be measured directly regardless of the dimensionality of the samples. The magnitude as well as the functional dependence of the corrections, obtained from the experiment, agree quantitatively with the theory. The data also show dimensinal crossover when the physical dimension of the samples is comparable to the length scale set by the thermal diffusion length. The crossover temperatures calculated from the theory agree quantitatively with those observed in the experiment.

The sample-size dependences of the electron-electron interactions can be conceptually understood using the following physical picture. In a weakly disordered system, the electron motion is diffusive in temporal and spatial scales large, compared to τ and l_e, respectively. The diffusive motion introduces two effects on the electron-electron interactions. First, the electrons under diffusion move away from each other much more slowly than in an ordered system, which leads to an increase of the duration of interactions. Second, in a disordered system, total momentum of the electrons is not conserved during the mutual interactions. This momentum nonconservation leads to a diffusive interaction correction to the conductivity of the electrons. The characteristic length of the diffusive interaction can be obtained by the following argument. In a system at T, an electron has an uncertainty in energy of order kT and an uncertainty in time $\hbar/kT$. In this time duration, the electron diffusively spreads out to a length $\Delta L=(\hbar D/kT)^{1/2}$, which is the uncertainty in the location of the diffusing electron. We can think of the electron as diffusively confined by the impurities within a length ΔL in a large sample. Associated with ΔL, the uncertainty in momentum is given by $\Delta p=\hbar/\Delta L$. Therefore, the total momentum of the interacting electrons need not be conserved within $q_{\max}\approx\hbar/\Delta L$, where q is the momentum transfer during the mutual interactions. When $W<\Delta L$, the electrons are confined by the physical size of the sample along the width, instead of by the impurities. As the width decreases, the electrons are more confined to each other and, at the same time, the uncertainty in the momentum increases. Consequently, the interactions become stronger. This leads to an increase of the magnetoresistance before the boundary scattering sets in to limit the orbital effect. For samples with short probe spacings, the diffusion along the channel is not disturbed. The short spacings only filter out the long-range interactions (i.e., small q) and, at low T, lead to a reduction of the magnetoresistance when compared with that from samples with the long probe spacings.

In this experiment we also observed other transport characteristics specific to the narrow channels. In the narrow channels with high mobilities, boundary scattering plays an important role. The scattering reduces all the orbital effects and leads to a new magnetoresistance, unexpected from the classical theory for a wide channel. The exact role of the boundary scattering in a narrow sample deserves further investigations. When the sample is both short and narrow, fluctuations of order e^2/h are observed. This observation shows that the sample is in a new regime where ensemble averaging does not exist.

Although the interaction theory in the weak-coupling regime is successful in this temperature regime ($T>1.25$ K), extending the measurements to lower temperatures (≈ 0.5 K) shows the magnetoresistance saturates even for the long channels. For example, extending the measurements on sample no. 7 to 0.5 K and fitting the data to Eq. (11) yields $L\approx 10$ μm (which corresponds to $T_{c2}\approx 0.75$ K) instead of its physical length 59 μm. This observation raises two possibilities: either there is a fundamental length cutoff in the theory suggested by Castellani *et al.*,[8] or there is a length scale set by the samples, such as the length scale of the macroscopic inhomogeneities, larger than which the electrons are not diffusively correlated. The former case implies that the mean size of the pseudo-local-spin moment is 10 μm. On the other hand, the macroscopic inhomogeneities, such as a small electron density gradient, have been detected in the measurements of quantum Hall effect.[43,44] The diffusion corrections in the presence of such macroscopic inhomogeneities need further investigation.

In the temperature range of this experiment ($\approx$4.2—to 1.2 K), the quantity $kT\tau_{tr}/\hbar$ is from 5.6 to 1.7. On the other hand, the theoretical calculation is done for $kT\tau/\hbar<1$. One possible explanation of the agreement of the present experiment and the theory is that the transport time τ_{tr} is much larger than the impurity scattering time τ due to the long-range nature of the scattering potential in the heterostructures.[45] However, the predictions of the interaction theory are also verified in the $kT\tau/\hbar>1$ regime even in systems known to have short-range scatterers, such as in copper[14] and in Si inversion layers.[32] Therefore, it is possible that the present results of the interaction theory are indeed applicable even in the $kT\tau/\hbar>1$ regime.

We have seen that reducing the width or the length of the sample changes the characteristics of the magnetoresistance at low B fields. More dramatic changes are observed when the measurements on these small samples are extended to high B fields. In the quantum Hall regime, the quantum oscillations of ρ_{xx} become sawtoothed and the peak values decrease drastically. In addition, the temperature dependence is totally different from that of a wide channel. Detail experimental results on narrow channels[46] and short channels[47] have been reported. Although perturbative calculations[48,49] for the electron-electron interactions exist in this regime and may explain some of the experimental features, the exact role of the electron-electron interactions, as well as the boundaries, in this high-field regime, still await further investigations.

ACKNOWLEDGMENTS

We thank R. Brown of RCA Laboratories for his help in mask making. The work at Princeton University is supported by the National Science Foundation through Grant No. DMR-82-12167.

*Present address: AT&T Bell Laboratories, Murray Hill, NJ 07974.

†Present address: Lincoln Laboratory, Massachusetts Institute of Technology, Lexington, MA 02173.

[1]P. Nozières and D. Pines, *Theory of Quantum Liquids* (Benjamin, New York, 1966).

[2]D. Forster, *Hydrodynamic Fluctuations, Broken Symmetry and Correlation Functions* (Benjamin/Cummings, Reading, 1975).

[3]B. L. Altshuler and A. G. Aronov, Zh. Eksp. Teor. Fiz. **77**, 2028 (1979) [Sov. Phys.—JETP **50**, 968 (1979)].

[4]For a review, see P. A. Lee and T. V. Ramakrihnan, Rev. Mod. Phys., **57**, 287 (1985).

[5]A. M. Finkel'stein, Zh. Eksp. Teor. Fiz. **84**, 168 (1983) [Sov. Phys.—JETP **57**, 97 (1983)].

[6]A. M. Finkel'stein, Zh. Eksp. Teor. Fiz. **86**, 397 (1984) [Sov. Phys.—JETP **59**, 212 (1984)].

[7]C. Castellani, C. Di Castro, P. A. Lee, and M. Ma, Phys. Rev. B **30**, 527 (1984).

[8]C. Castellani, C. Di Castro, P. A. Lee, M. Ma, S. Sorella, and E. Tabet, Phys. Rev. B **30**, 1596 (1984).

[9]For a brief review, see B. L. Altshuler and A. G. Aronov, *Electron-Electron Interactions in Disordered Systems,* edited by M. Pollak and A. L. Efros (North-Holland, Amsterdam, 1984).

[10]A. E. White, R. C. Dynes, and J. P. Garno, Phys. Rev. B **31**, 1174 (1984).

[11]M. E. Gershenzon, V. N. Gubankov, and M. I. Falei, Pis'ma Zh. Eksp. Teor. Fiz. **41**, 435 (1985) [JETP Lett. **41**, 534 (1985)].

[12]D. J. Bishop, D. C. Tsui, and R. C. Dynes, Phys. Rev. Lett. **44**, 1153 (1980).

[13]Y. Kawaguchi and S. Kawaji, J. Phys. Soc. Jpn. **48**, 699 (1980).

[14]A. E. White, M. Tinkham, W. J. Skoçpol, and D. C. Flanders, Phys. Rev. Lett. **48**, 1752 (1982).

[15]J. T. Madsen and N. Giordano, Phys. Rev. Lett. **49**, 819 (1982).

[16]M. Lavion, P. Auerbuch, H. Godfrin, and R. E. Rapp, J. Phys. Lett. **44**, L1021 (1983).

[17]D. J. Bishop, R. C. Dynes, and D. C. Tsui, Phys. Rev. B **26**, 773 (1982).

[18]R. A. Davis, M. J. Uren, M. Kaveh, and M. Pepper, J. Phys. C **14**, 5737 (1981).

[19]B. L. Altshuler, D. Khmelnitzkii, A. I. Larkin, and P. A. Lee, Phys. Rev. B **22**, 5142 (1980).

[20]M. A. Paalanen, D. C. Tsui, and J. C. M. Hwang, Phys. Rev. Lett. **51**, 2226 (1983).

[21]K. K. Choi, D. C. Tsui, and S. C. Palmateer, Phys. Rev. B **32**, 5540 (1985).

[22]K. K. Choi, D. C. Tsui, and S. C. Palmateer, in Proceedings of the Sixth International Conference on Electron Properties of the Two Dimensional Systems, Kyoto, Japan, 1985, edited by T. Ando (unpublished).

[23]H. Fukuyama, Y. Isawa, and H. Yasuhara, J. Phys. Soc. Jpn. **52**, 16 (1983).

[24]B. L. Altshuler and A. G. Aronov, Solid State Commun. **46**, 429 (1983).

[25]B. L. Altshuler, A. G. Aronov, and A. Yu Zyuzin, Zh. Eksp. Teor. Fiz. **86**, 709 (1984) [Sov. Phys.—JETP **59**, 415 (1984)].

[26]K. Scharnberg, in Proceedings of the International Conference on Localization, Interaction and Transport Phenomena in Impure Metals, Braunschweig, Aug. 23, 1984, supplement (unpublished).

[27]B. L. Altshuler, A. G. Aronov, A. I. Larkin, and D. E. Khmelnitskii, Zh. Eksp. Teor. Fiz. **81**, 768 (1981) [Sov. Phys.—JETP **54**, 411 (1981)].

[28]H. Fukuyama, J. Phys. Soc. Jpn. **50**, 3407 (1981).

[29]M. Kaveh, M. J. Uren, R. A. Davies, and M. Pepper, J. Phys. C **14**, L413 (1981).

[30]R. G. Wheeler, K. K. Choi, A. Goel, R. Wisnieff, and D. E. Prober, Phys. Rev. Lett. **49**, 1674 (1982).

[31]S. Hikami, A. I. Larkin, and Y. Nagaoka, Prog. Theor. Phys. **63**, 707 (1980).

[32]K. K. Choi, Phys. Rev. B **28**, 5774 (1983).

[33]A. Houghton, J. R. Senna, and S. C. Ying, Phys. Rev. B **25**, 2196 (1982).

[34]P. A. Lee and T. V. Ramakrishnan, Phys. Rev. B **26**, 4009 (1982).

[35]Th. Englert, D. C. Tsui, A. C. Gossard, and Ch. Uihlein, Surf. Sci. **113**, 295 (1982).

[36]T. Ando, J. Phys. Soc. Jpn. **37**, 1233 (1974).

[37]W. J. Skoçpol, L. D. Jackel, R. E. Howard, P. M. Mankiewich, D. M. Tennant, A. E. White, and R. C. Dynes, in Proceedings of the Sixth International Conference on Electron Properties of Two Dimensional Systems, Kyoto Japan, 1985, Ref. 22, p. 1.

[38]A. B. Fowler, A. Harstein, and R. A. Webb, Phys. Rev. Lett. **48**, 196 (1982).

[39]R. A. Webb, S. Washburn, C. P. Umbach, and R. B. Laibowitz, Phys. Rev. Lett. **54**, 2696 (1985).

[40]P. A. Lee and A. D. Stone, Phys. Rev. Lett. **55**, 1622 (1985).

[41]B. L. Altshuler, Zh. Eksp. Teor. Fiz. **41**, 530 (1985) [Sov.

Phys.—JETP **41**, 648 (1985)].
[42]H. Sakaki, H. Hirakawa, J. Yoshino, S. P. Svensson, Y. Sekizuchi, T. Motta, S. Nishi, and N. Miura, Surf. Sci. **142**, 306 (1984).
[43]G. Ebert, K. v. Klitzing, and G. Weimann, J. Phys. C **18**, L257 (1985).
[44]H. Z. Zheng, D. C. Tsui, and A. M. Chang, Phys. Rev. B **32**, 5506 (1985).
[45]S. Das Sarma and F. Stern, Phys. Rev. B **32**, 8442 (1985).
[46]H. Z. Zheng, K. K. Choi, D. C. Tsui, and G. Weimann, Phys. Rev. Lett. **55**, 1144 (1985).
[47]H. Z. Zheng, K. K. Choi, D. C. Tsui, and G. Weimann, in Proceedings of the Sixth International Conference on the Electron Properties of Two Dimensional Systems, Kyoto, Japan, 1985, Ref. 22, p. 261.
[48]S. M. Givin, M. Jonson, and P. A. Lee, Phys. Rev. B **26**, 1651 (1982).
[49]A. Houghton, J. R. Senna, and S. C. Ying Phys. Rev. B **25**, 6468 (1982).